Plant Pathology (2011) Doi: 10.1111/j.1365-3059.2011.02466.x

Spatial characteristics of white mould epidemics and the development of sequential sampling plans in Australian bean fields

S. J. Jones[a], D. H. Gent[b], S. J. Pethybridge[c] and F. S. Hay[a]*

[a]*Tasmanian Institute of Agricultural Research (TIAR), University of Tasmania, PO Box 3523, Burnie, Tasmania 7320, Australia;* [b]*United States Department of Agriculture-Agricultural Research Service, Forage Seed and Cereal Research Unit, Oregon State University, Department of Botany and Plant Pathology, Corvallis, OR 97331, USA; and* [c]*Botanical Resources Australia – Agricultural Services Pty Ltd, PO Box 3251, Ulverstone, Tasmania 7315, Australia*

To improve sampling efficiency and precision in the assessment of white mould (caused by *Sclerotinia sclerotiorum*) disease incidence on bean (*Phaseolus vulgaris*), the spatial characteristics of epidemics were characterized in 54 linear transects in 18 bean fields during 2008–2010 in northern Tasmania, Australia. The incidence of diseased pods and plants was assessed prior to harvest. Distributional and correlation-based analyses indicated the incidence of diseased pods was characterized by a largely random pattern at the individual plant scale, with some patches of similar disease levels on pods occurring at a scale of 1·5 m or greater. Collectively, these results suggested epidemics may be dominated by localized sources of inoculum. Sequential sampling approaches were developed to estimate or classify disease incidence above or below provisional thresholds of 3, 5 and 15% incidence on pods near harvest. Achieving prespecified levels of precision by sequential estimation was possible only when disease incidence on pods was greater than approximately 4% and sampling was relatively intense (i.e. 10 pods evaluated on each of at least 64 plants). Using sequential classification, correct decisions on disease status were made in at least 95% of independent validation datasets after assessment of only 10·1–15 plants, depending on classification threshold and error rates. Outcomes of this research provide the basis for implementing more efficient sampling and management strategies for this disease in Australian fields.

Keywords: epidemic development, *Phaseolus vulgaris*, sampling precision, *Sclerotinia sclerotiorum*, white mould

Introduction

White mould (*Sclerotinia sclerotiorum*) causes substantial annual losses of bean (*Phaseolus vulgaris*) production worldwide (Boland & Hall, 1987). The disease may affect all aerial plant parts and can reduce the number and size of pods, cause pods to rot and kill entire plants (Wong, 1978). Early symptoms include water-soaked areas on stems, leaves or pods, which develop into soft, pale-brown lesions. White cottony mycelia are then formed on lesions, and as the tissue senesces, mycelial mounds are formed which mature into hard, melanized, black sclerotia (approximately 5–10 mm long) which allow the fungus to survive in a dormant state for periods of months or years (Willetts & Wong, 1980; Koike *et al.*, 2007). Moreover, infection of the stem can cause weakening and result in losses through lodging (Boland & Hall, 1987).

Sclerotinia sclerotiorum has a wide host range, including crops routinely used in rotation with bean in Tasmania, Australia (and elsewhere), including carrot, potato, pea, alkaloid poppy and pyrethrum. Several weed species commonly encountered in bean fields are also susceptible hosts of this fungus (Wong, 1978; Boland & Hall, 1988; McDonald & Boland, 2004). Disease outbreaks in these crops and weeds can contribute to increases in inoculum density over time. The ability of *S. sclerotiorum* to survive for long periods in soil as sclerotia (Willetts & Wong, 1980; Koike *et al.*, 2007), combined with the ability of sclerotia to produce large quantities of windborne ascospores (Schwartz & Steadman, 1978; Phillips, 1987; Clarkson *et al.*, 2004), the broad host range of the pathogen, and the absence of high levels of host plant resistance in bean, make white mould particularly difficult to control.

Sclerotia of *S. sclerotiorum* can undergo either myceliogenic or carpogenic germination (Abawi *et al.*, 1975; Abawi & Grogan, 1979). In the white mould–bean pathosystem, myceliogenic germination of sclerotia is believed to be of minor concern in Australian bean crops. Most yield losses are attributed to carpogenic germination and subsequent infection of senescent flowers and withered leaves (Schwartz & Steadman, 1978; Wong, 1978; Phillips, 1987; Clarkson *et al.*, 2004). Ascospores

*E-mail: Frank.Hay@utas.edu.au

require high humidity and nutrients from senescent or damaged tissue to germinate and initiate infection (Phillips, 1987; McCartney & Lacey, 1991). In beans, senescing petals are particularly susceptible to infection. In several pathosystems, carpogenic germination of *S. sclerotiorum* has been modelled to be synchronous with the availability of host tissue (i.e. flower development) (Abawi *et al.*, 1975; Abawi & Grogan, 1979; Boland & Hall, 1988; Pethybridge *et al.*, 2010). However, temperature, water potential and light interception have been documented as the most important factors regulating carpogenic germination (Schwartz & Steadman, 1978; Huang & Kozub, 1993; Turkington & Morall, 1993; Clarkson *et al.*, 2004; McDonald & Boland, 2004). Secondary spread occurs when infected petals fall through the canopy and attach to pods, leaves or stems. Mycelia can then grow from the petals and infect healthy plant parts, such as stems and pods (Abawi *et al.*, 1975; Abawi & Grogan, 1979).

Current management of white mould on beans relies mainly on the prophylactic use of fungicides at the flowering stage. The aim of this programme is to prevent initial ascospore infection of senescing flowers and consequently to reduce secondary infection of healthy plant tissues. The decision to implement a management strategy based on an action threshold requires a sampling procedure that is capable of accurately estimating disease incidence or classifying incidence as being above or below a specified value (Binns *et al.*, 2000). Sequential sampling methods have been developed and used widely in entomology to minimize time and costs associated with assessing arthropod pest density (e.g. Hoffman *et al.*, 1996), but have been less used in assessing plant disease. Examples of the latter include common maize rust (Dillard & Seem, 1990), yellow (stripe) rust of wheat (Gaunt & Cole, 1992), phomopsis leaf blight of strawberry (Turechek *et al.*, 2001), botrytis leaf blight of onion (Vincelli & Lorbeer, 1987) and powdery mildew of hop (Gent *et al.*, 2007a,b). The development of a sequential sampling plan requires prior knowledge of the spatial pattern of disease. Sequential sampling can be of two forms: (i) sequential estimation, in which it is necessary to estimate the level of disease at a particular level of precision, or (ii) sequential classification, which seeks to determine whether disease is above or below a critical value important for disease management. At disease incidences higher or lower than the critical value, disease can be classified with fewer samples than when the incidence is near the critical value. In general, sequential sampling plans based on classification require less intensive sampling than those based on estimation because precision is not controlled at all levels of disease incidence and sampling ceases when enough individuals have been assessed to simply classify disease status (Madden *et al.*, 1996, 2007; Madden & Hughes, 1999; Binns *et al.*, 2000).

In some cases with plant diseases, sequential sampling has been used to initiate fungicide applications (Vincelli & Lorbeer, 1987). However, in the case of white mould of bean, the use of a sequential sampling plan for scheduling fungicides for disease management may be of limited value. In this pathosystem, fungicides need to be applied at flowering, some weeks prior to the onset of symptoms on plants. Similarly, treatment of pods with fungicides may be less efficacious than treatment of flowers, and treatment of pods may lead to an inadequate withholding period prior to harvest. Furthermore, the latent period between infection and disease expression may mean that at the point of detection, the disease has already increased to the point that economic management is not possible (Malloy, 1993).

The major potential benefit of a sequential sampling plan for white mould in bean is improving the efficiency of assessing disease incidence within fields for processors to determine if disease incidence is too high for a field to be harvested. In this study, the objectives were to quantify the spatial patterns of white mould epidemics in Australian bean fields, and to use this information to derive sequential sampling plans for estimation and classification of the incidence of pods with white mould.

Materials and methods

Field trials and data collection

The incidence of white mould on bean pods was quantified in surveys of 18 commercial bean fields on undulating terrain in northern Tasmania, Australia during 2008–2010. A total of five, six and seven fields were assessed in 2008, 2009 and 2010, respectively. The incidence of diseased pods was assessed using a cluster sampling design, which is necessary to assess aggregation with disease incidence data (Hughes *et al.*, 1996). For each field, two to four rows were selected, and a linear transect was established on the selected rows. Each transect was 50 m long and disease incidence was assessed in quadrats (sampling units) 0·5 m long by one row wide, for a total of $N = 100$ sampling units per transect. From each sampling unit, $n = 10$ pods (individuals) were selected randomly and assessed for signs and symptoms of white mould. Thus, there were a total Nn pods evaluated per transect. Estimated disease incidence ($\hat{p}$) was then calculated as $\hat{p} = \sum x_i / \sum n_i$, where x_i is the number of diseased pods and n_i is the number of pods sampled in the ith sampling unit. Each transect was considered a dataset, resulting in a total of 54 datasets for model development (herein referred to 'model development datasets').

An additional 109 bean fields were assessed for white mould during 2009 and 2010. These datasets were considered independent 'model validation datasets' and were used to assess the performance of the sequential sampling plans described below. In these assessments, fields were assessed for white mould as close to commercial harvest as practical, which was generally 2–10 days before harvest. When assessing disease incidence in these fields, pods and plants at 64 points in the field were assessed for white mould. The 64 sampling points consisted of four or five transects each with 12–16 relatively equally spaced points that spanned the length of the field. At each

sampling point, 20 pods were selected arbitrarily from one to two bean plants. This was analogous to the commercial protocols used by processors to estimate disease incidence within fields.

Spatial analyses

Distributional analyses

The beta-binomial and binomial distributions were fitted to the incidence of diseased pods and plants using the computer program BBD (Madden & Hughes, 1994). A good fit to the binomial distribution is an indication of a random pattern of diseased pods, whereas a good fit to the beta-binomial distribution is an indication of an aggregated pattern (Madden & Hughes, 1995; Madden *et al.*, 2007). A log-likelihood ratio test was conducted to determine whether the data was a better fit to the beta-binomial distribution or the binomial distribution. The $C(\alpha)$ test also was used to test whether aggregation in the distribution of diseased pods could be described adequately by the beta-binomial distribution. Since 20 pods per sampling unit were assessed for white mould in the model validation datasets, 10 pods were selected randomly from among the 20 pods assessed *post hoc* in an Excel spreadsheet before conducting distributional analysis on the model validation datasets.

The degree of aggregation of disease incidence was quantified by the heterogeneity parameter θ of the beta-binomial distribution, which is a measure of spatial heterogeneity of disease per sampling unit (Madden & Hughes, 1995; Madden *et al.*, 2007). The index of dispersion (D) was calculated by dividing the observed variance of diseased pods (v_{obs}) by the theoretical variance for a binomial distribution (v_{bin}), where $v_{obs} = \left[\sum (x_i - \hat{p}n_i)^2\right]/(N-1)$ and $v_{bin} = n\hat{p}(1-\hat{p})$ and x_i, $\hat{p}$, n and N are as defined previously. When $\theta = 0$ or $D = 1$, the pattern of diseased pods is interpreted as random, with aggregation indicated when $D > 1$ or $\theta > 0$ and the degree of aggregation directly proportional to the magnitude of the statistic. D has a chi-square distribution, and was used to test a null hypothesis of a random distribution of disease incidence with $N - 1$ degrees of freedom (Madden & Hughes, 1995).

Binary power law analyses

The binary power law expresses the relationship between the variance of a theoretical variance of binomial (random) pattern of disease incidence and an observed variance (Hughes & Madden, 1992). When a large number of datasets are collected, the relationship between these variances provides a convenient means to characterize aggregation of disease incidence over multiple fields and time (Madden *et al.*, 2007; Gent *et al.*, 2008). The model was fitted to the observed and binomial variances through the log-transformed relationship

$$\ln(v_{obs}) = \ln(A_x) + b\ln(v_{bin}) \qquad (1)$$

where v_{obs} and v_{bin} are as defined above. When $A_x = 1$ and $b = 1$, Eqn 1 indicates a random pattern of disease incidence that can be represented by the binomial distribution. When $A_x > 1$ and $b = 1$, disease incidence has an aggregated pattern that is not dependent on p; values of $b > 1$ indicate that aggregation is systematically related to p. Ordinary least squares regression was used to estimate the intercept and slope parameters using PROC REG in SAS version 9.2 (SAS Institute).

Correlation-based spatial analyses

Correlation-based spatial analyses for the incidence of diseased pods were conducted using autocorrelation and both ordinary and median runs analyses. First- and second-order autocorrelation statistics were calculated to quantify the degree of similarity of disease incidence between sampling units along a transect. Before autocorrelation coefficients were calculated, the data were transformed using the Haldane transformation $[\ln(y/(1-y)]$, where $y = (x + 0{\cdot}5)/(n+1)$ and x is the number of diseased pods in a sampling unit. This transformation avoids taking the logarithm of 0 values or dividing by 0. Autocorrelation analyses were performed in Minitab version 15 (Minitab, Inc.).

Ordinary and median runs analyses were performed to characterize larger-scale patterns of diseased pods among sampling units in a transect (Madden *et al.*, 1982). For ordinary runs analysis, a sampling unit was assigned a value of 1 if at least one diseased individual was observed in the sampling unit and a 0 otherwise. In median runs analysis, the median incidence of disease was calculated for each dataset. Sampling units were then coded as 1 or 0 if the incidence of diseased pods was above or below the median for that dataset, respectively. A run was defined as a succession of one or more sampling units with similar disease status (non-diseased or diseased). Runs and associated tests of significance were calculated in Minitab.

Sequential sampling curves

Sequential estimation

A full explanation of the methods and theory for sequential sampling is given in the literature citations below (e.g. Madden *et al.*, 1996) and hence only a brief explanation is given here. Binary power law parameters estimated from the model development datasets were used in the development of sequential estimation models. Precision was expressed in terms of the coefficient of variation, $C = SE\hat{p}/\hat{p}$, where SE is the standard error. The SE of $\hat{p}$ was expressed in terms of the binary power law parameters as:

$$\sqrt{a[\hat{p}(1-p)]^b/N} \qquad (2)$$

where $a = A_x n^{b-2}$.

In sequential sampling for estimation, the cumulative number of diseased pods over N sampling units, T_N, is tallied after each sampling unit is assessed. Sampling ceases when T_N reaches or exceeds a threshold value, referred to as the stop limit, which is defined by a, b, n, N and C. Disease incidence is then calculated as $\hat{p} = T_N/nN$. The stop lines can be calculated exactly for a binomial

distribution (i.e. $\theta = 0$) or approximated numerically when disease is aggregated and the degree of aggregation varies systematically with disease incidence (i.e. values of $b > 1$) by:

$$\gamma_N = T_N^{b-2}(nN - T_N)^b = (C^2/a)n^{2b-2}N^{2b-1} \quad (3)$$

where γ_N is a function of T_N. A Mathcad (Mathsoft Inc.) worksheet developed by Turechek *et al.* (2001) was used to solve Eqn 3 iteratively for T_N when $N = 1$ to 500 and $C = 0{\cdot}1$, $0{\cdot}2$ and $0{\cdot}3$ as explained previously (Gent *et al.*, 2007a,b).

Sequential classification

Statistical methods used for development of the sequential classification models were based on a modified version of Wald's sequential probability ratio test (SPRT), as explained in depth by Madden & Hughes (1999). For sequential classification, $p_t = (p_0 + p_1)/2$ is defined as some critical value of disease incidence, which in this study was the threshold for processor rejection of beans as a result of white mould. The parameters p_0 and p_1 represent the lower and upper boundaries of disease incidence such that, when the true incidence of disease, p, is equal to or less than p_0, the field is classified correctly at least $100(1 - \alpha)\%$ of the time; and when the true incidence of disease is equal to or greater than p_1, the field is classified correctly at least $100(1 - \beta)\%$ of the time. In practice, the resulting classifications are interpreted as a test of the null hypothesis H_0: $p \leq p_t$ against the alternative hypothesis H_1: $p > p_t$, respectively. A type I error is made when the true disease incidence, p, is incorrectly classified as greater than the critical value, p_t. A type II error is made when p is incorrectly classified as less than p_t. The rate of these two errors is expressed by the operating characteristic (OC; explained thoroughly in Binns *et al.*, 2000), which is defined as the probability of accepting the null hypothesis given the true value of p. The OC = 1 − (type I error rate) when $p \leq p_t$, and is the type II error rate when $p > p_t$. The OC of a perfect sampling plan is 1 when $p \leq p_t$ and 0 when $p > p_t$; the steepness of an OC provides an indication of the error rate of a sampling plan. Plots of average sample number (ASN) versus p are also used to evaluate the properties of sequential classification sampling plans. The ASN is the expected number of sampling units that need to be examined in order to accept or reject the null hypothesis for any true value of p. The OC and ASN provide the expected (average) values over many samplings, and not necessarily the performance of a sampling plan for an individual field. A steep OC and low ASN are desirable for sequential sampling because these indicate low error rates and efficient sampling plans.

With sequential classification, two stop lines are calculated to represent p_0 and p_1. The exact calculation of stop lines for the SPRT is not possible for data described by the beta-binomial distribution, but approximate formulae are available (Madden & Hughes, 1999). The general formula for stop lines is:

$$i_0 + snN < T_N < i_1 + snN \quad (4)$$

where sn is the common slope of the stop lines, and i_0 are i_1 are intercepts of the lower and upper stop lines, respectively. Intercept terms are defined by a, b, p_0, p_1 and error parameters analogous to type I (α) and type II (β) errors (Madden & Hughes, 1999; Turechek *et al.*, 2001).

In this study, sequential classification thresholds were based on three levels of p_t: $0{\cdot}03$ ($p_0 = 0{\cdot}01$, $p_1 = 0{\cdot}05$); $0{\cdot}05$ ($p_0 = 0{\cdot}03$, $p_1 = 0{\cdot}07$); and $0{\cdot}15$ ($p_0 = 0{\cdot}088$, $p_1 = 0{\cdot}214$). These values of p_t were selected based upon processor rejection thresholds for white mould of approximately 5% incidence. The sampling plan with $p_t = 0{\cdot}03$ would be a conservative approach to ensuring that most fields would be classified as <0·05. The value of $p_t = 0{\cdot}15$ was derived from a regression equation describing the relationship between in-field disease incidence assessments and those of the co-operating processor ($y = 0{\cdot}32x + 0{\cdot}174$, where y = disease incidence as estimated by the processor and x = disease incidence estimated during field surveys; $n = 32$ fields; $R^2 = 0{\cdot}73$). In these studies, $\hat{p} = 0{\cdot}15$ estimated from the surveys corresponds roughly to $\hat{p} = 0{\cdot}05$ as estimated by the processor. Each of these threshold values were evaluated at α and β error rates of 0·05 and 0·10. Thus, six sampling plans were developed and evaluated by plots of OC and ASN versus p. OC and ASN were calculated by MonteCarlo simulations using a Fortran program developed by J. P. Nyrop and modified by L. V. Madden (Turechek *et al.*, 2001).

Sampling plan validation by simulated sampling

Sequential estimation

Validation is an important aspect of developing sampling plans to ensure they perform as desired during routine use. Sampling plans were validated with the 109 independent validation datasets by simulated sampling using a Minitab macro (described by Turechek *et al.*, 2001 and Gent *et al.*, 2007a). For a given dataset, the sampling units were entered into the macro in the same order they were collected in the field. The macro simulated sampling of diseased pods collected from the sampling units, and tallied the cumulative number of diseased pods until the cumulative number of diseased pods exceeded that of the model T_N calculated from Eqn 3. Estimates of p, the achieved C, and the achieved N were then calculated. Datasets where incidence of disease was 0 were not used for determining the achieved C. The data were summarized in box plots and the distribution of the median value of the difference between the true and achieved p, achieved C, and N were compared by the nonparametric sign test in Minitab (Ryan *et al.*, 2005).

Sequential classification

The six sequential classification sampling plans selected after MonteCarlo simulation were evaluated by simulated sampling of the model validation datasets as

described for sequential estimation. Stop lines were calculated based on either the binomial distribution or beta-binomial distribution. To determine if a correct decision for a dataset was made, it was assumed that the observed p from all 64 sampling units in a field represented the 'true' p for that field. The true value of p for a dataset was compared with the hypothesized p_t to determine whether to reject the H_0 in favour of the H_1. The decision based on results of the simulated sequential classification was compared to the correct decision for the field, in order to calculate type I and type II error rates. A type I error was recorded if mean disease incidence was incorrectly classified as greater than p_t, and a type II error was recorded if mean disease incidence was incorrectly classified as less than p_t.

Sampling plan evaluation by bootstrapping

Sequential estimation

Evaluation of the sequential sampling plans was also conducted by bootstrap evaluation of 12 datasets that encompassed the range of $\hat{p}$ observed among the model development datasets. The 54 model development datasets were classified into four disease incidence categories that spanned the range of disease incidence observed:

$$0{\cdot}02 < \hat{p} < 0{\cdot}04, 0{\cdot}05 \leq \hat{p} < 0{\cdot}08, 0{\cdot}08 \leq \hat{p} < 0{\cdot}16, \text{ and } \hat{p} \geq 0{\cdot}16.$$

Three datasets were selected randomly from each disease incidence class for bootstrap evaluation. For a given bootstrap simulation, sampling units (n = 10 pods from a quadrat) were sampled randomly one at a time, with replacement, from among all sampling units in a transect. Predicted stop limit curves for sequential estimation were determined according to Eqn 3 with C = 0·1 and C = 0·2, and binary power law parameters a = 0·194 and b = 1·045. Bootstrap analysis was conducted using a macro executed in Minitab to calculate the achieved C, the difference between the p of the dataset (true p) and achieved p using sequential sampling for estimation, and the achieved N for each of the 12 datasets. A rule was implemented that a minimum of 10 sampling units were collected before sampling ceased to ensure a representative sample was collected. The bootstrap evaluation was conducted 100 times for each dataset and specified values of C.

Sequential classification

The six sequential classification sampling plans were evaluated by bootstrap simulation, as described above for sequential estimation. Stop lines were determined using Eqn 4. Sampling ceased when the cumulative number of diseased pods exceeded the upper or lower stop lines of the model, or the dataset was sampled fully. Again, a minimum of 10 sampling units were collected before sampling ceased to ensure a representative sample was collected. The bootstrap simulation was conducted 100 times for each dataset and specified values of p_t, p_0, p_1, α and β, and achieved OC and ASN were then calculated.

Results

Disease incidence

The incidence of pods with white mould determined from the disease surveys ranged from 2·8% to 23·1% among fields assessed, with a median of 8·4%. Among the model validation datasets, disease incidence on the pods ranged from 0% to 13·8% with a median of 0·2%.

Spatial analyses

Distributional analyses

All spatial analyses, at the scale of individual sampling units, indicated that disease incidence was slightly aggregated in the model development datasets (Fig. 1; Table 1). The log-likelihood ratio test was significant for 83% of the datasets, indicating that the beta-binomial distribution provided a better fit to the data than the binomial (random) distribution. Similarly, the $C(\alpha)$ test indicated that the beta-binomial distribution provided a better fit than the binomial distribution for 93% of datasets. The frequency distribution of the heterogeneity parameter $\hat{\theta}$ was highly right-skewed and ranged from 0·0042 to 0·37 with median 0·10, which indicated a low degree of aggregation (Fig. 1b; Table 1). The frequency distribution of the index of dispersion, D, ranged from 1·05 to 3·48 with median 1·80 (Fig. 1c). In 91% of the datasets D was greater than 1 (suggesting significant aggregation) according to a chi-square test.

In the model validation datasets, disease incidence was randomly distributed on pods within sampling units. The heterogeneity parameter ranged from 0 to 0·27 with median 0, in datasets where $\hat{p} > 0$ (Fig. 2b). The index of dispersion ranged from 0·69 to 2·91, with median 1, indicating a random distribution of disease incidence (Fig. 2c).

Binary power law analyses

The binary power law provided a reasonable fit to the data in 2008 and 2009 (R^2 = 0·82 and 0·84, respectively), but a poor fit in 2010 (R^2 = 0·45; Fig. 3a). In each year, and averaged over all years, the intercept estimates were significantly greater than 0, but the slope parameter estimates were not significantly different from 1 (Table 2). This indicated that the incidence of diseased pods was aggregated (intercept greater than 0), but the degree of heterogeneity was independent of disease incidence (slope equal to 1).

In the model validation dataset on pods, disease incidence was significantly more aggregated than the model development datasets. The estimated parameters for the intercept and slope terms were significantly greater than 0 and 1 respectively, indicating aggregation that was systematically related to p (Table 2; Fig. 3b).

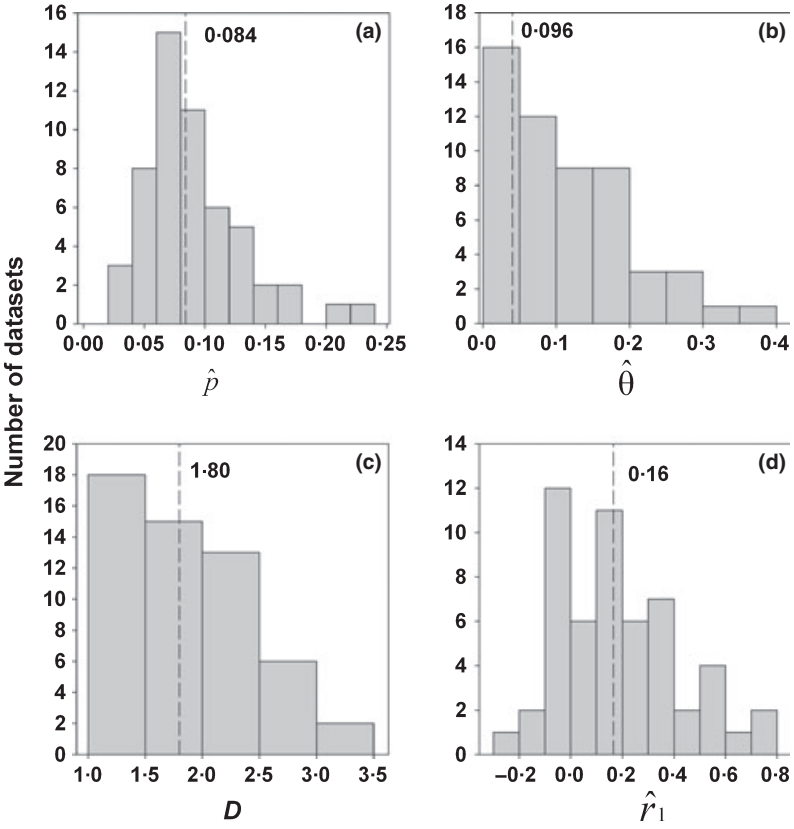

Figure 1 Frequency distribution of the beta-binomial distribution parameters $\hat{p}$ (a) and $\hat{\theta}$ (b), the index of dispersion D (c), and the first-order autocorrelation statistic $\hat{r}_1$ (d) for the incidence of bean pods with white mould (*Sclerotinia sclerotiorum*) as assessed in 54 transects in 18 commercial bean fields in Australia and used for sampling model development. Each vertical dashed line is the median value for the indicated statistic, with the numerical value given on the graph.

Table 1 Tests of aggregation and spatial pattern of incidence of bean pods with white mould (*Sclerotinia sclerotiorum*) sampled from commercial bean fields in Tasmania, Australia during 2008–2010

			Variance tests[d]		Median values[e]			Runs analysis[f]	
Incidence[a]	T[b]	LRS[c]	$C(\alpha)$	D	$\hat{\theta}$	D	$\hat{r}$	Median	Ordinary
>0·02–0·04	3	1·00	1·00	1·00	0·09	1·79	0·06	0·33	0·33
>0·04–0·08	23	0·74	0·91	0·87	0·06	1·54	0·08	0·26	0·26
>0·08–0·16	24	0·92	0·96	0·96	0·13	2·07	0·24	0·43	0·46
>0·16	4	0·75	0·75	0·75	0·11	1·86	0·09	1·00	0·25
All	54	0·83	0·93	0·91	0·10	1·80	0·16	0·37	0·35

[a]Incidence of pods with white mould in 54 datasets used for constructing sequential sampling models.
[b]Number of datasets in each disease incidence class.
[c]Proportion of datasets in which the likelihood ratio test statistic was significant ($P \leq 0{\cdot}05$).
[d]Proportion of datasets in which the $C(\alpha)$ (z-statistic) or D (chi-square) tests were significant ($P \leq 0{\cdot}05$).
[e]Median estimated value of the beta-binomial distribution parameter $\hat{\theta}$, index of dispersion D, and first-order autocorrelation statistic $\hat{r}$.
[f]Percentage of datasets in which runs analysis indicated significant aggregation. Ordinary runs analysis was based on 23 or two datasets in the disease incidence classes >0·08–0·16 and >0·16, respectively, because runs could not be calculated in some instances since all sampling units had at least one diseased pod.

Autocorrelation analyses

Significant first-order autocorrelation ($\hat{r}_1$) of disease incidence on pods was detected in 50% of the datasets, with significant second-order autocorrelation in 44% of datasets (Table 1). The frequency distribution of $\hat{r}_1$ ranged from −0·23 to 0·78 with median 0·16 (Fig. 1d). At lag = 2, median $\hat{r}_2$ was 0·15. Together, this indicates a low but significant level of aggregation of disease incidence in patches of about 1–1·5 m or greater.

Runs analyses

Significant aggregation was detected in 37% of the datasets by median runs analysis and 35% of the datasets where more than one run was present (Table 1), again indicating some patches of disease extending beyond the borders of individual sampling units. There was a tendency for median runs analysis to detect greater aggregation as disease incidence increased.

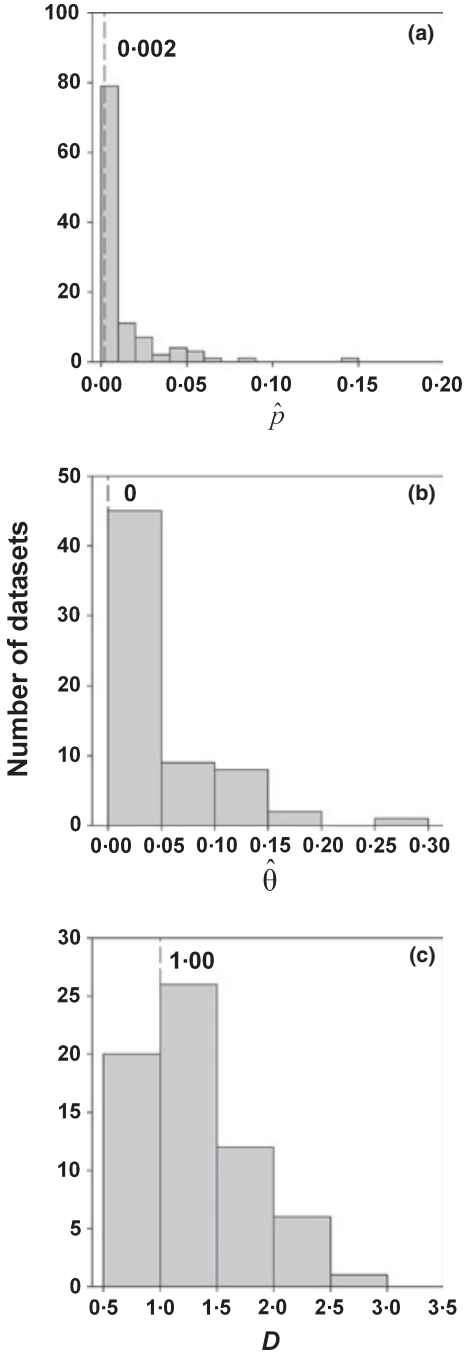

Figure 2 Frequency distribution of the beta-binomial distribution parameters $\hat{p}$ (a) and $\hat{\theta}$ (b), and the index of dispersion D (c) for the incidence of bean pods with white mould (*Sclerotinia sclerotiorum*) in Australian bean fields used for sampling model validation. (a) Datasets from 109 fields; (b and c) 65 datasets where disease incidence $\hat{p} > 0$. Each vertical dashed line is the median value for the indicated statistic, with the numerical value given on the graph.

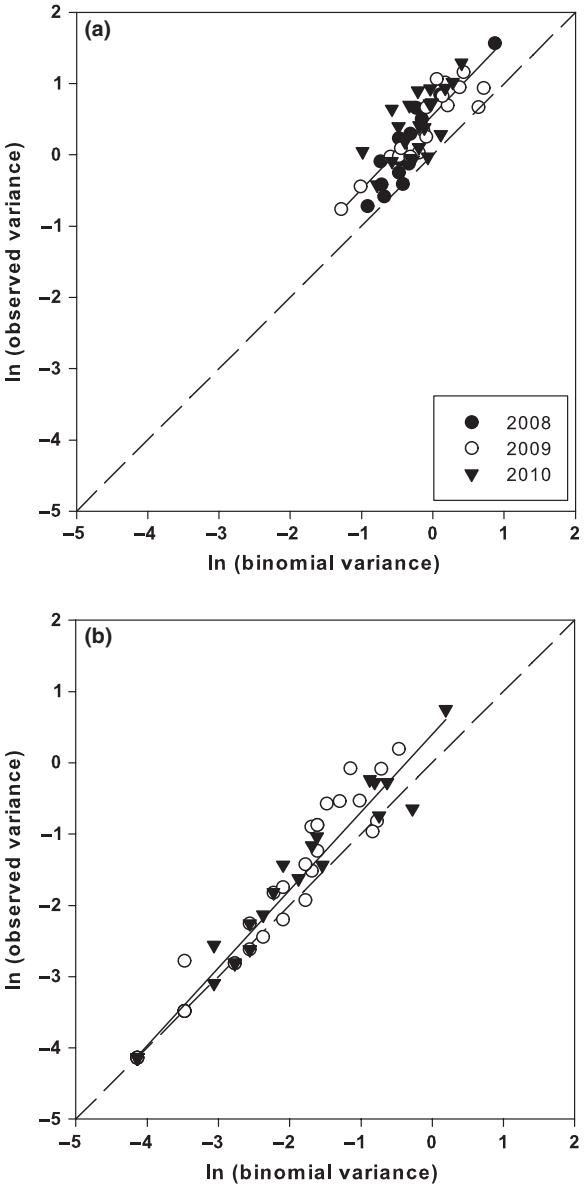

Figure 3 Relationship between the logarithms of the observed variance and binomial variance of the incidence of bean pods with white mould (*Sclerotinia sclerotiorum*) in Tasmania, Australia in model development datasets (a) and model validation datasets (b). The solid line is the least squares regression fit to data from 2008 (•), 2009 (○) and 2010 (▼); the dashed line represents a binomial (random) distribution of disease incidence. Slope and intercept parameter estimates are given in Table 2.

Sequential sampling curves

Sequential estimation

Sequential estimation stop limits for estimating mean incidence of pods with white mould and the corresponding disease incidence at T_N are shown in Fig. 4a and Fig. 4b, respectively, for C = 0·1, 0·2 and 0·3. As expected, increasing sampling precision or decreasing disease incidence resulted in a greater cumulative number of diseased individuals before sampling could cease.

Simulated sampling validation

There were 65 validation datasets where $p > 0$. In these datasets, estimates of disease incidence obtained by

Table 2 Estimated slope ($\hat{b}$) and intercept parameters (ln [$\hat{A}_x$]) of the binary power law fitted to the incidence of bean pods with white mould (*Sclerotinia sclerotiorum*) in commercial bean fields in Tasmania, Australia

	Model development datasets				Model validation datasets			
Year	df[a]	$\hat{b}$ (SE)[b]	ln ($\hat{A}_x$) (SE)[b]	R^2	df[a]	$\hat{b}$ (SE)[b]	ln($\hat{A}_x$) (SE)[b]	R^2
2008	13	1·316 (0·156)	0·555 (0·084)	0·84	…	…	…	…
2009	16	0·947 (0·113)	0·511 (0·059)	0·82	32	1·166 (0·047)	0·649 (0·124)	0·95
2010	19	0·899 (0·226)	0·625 (0·090)	0·45	29	1·090 (0·033)	0·399 (0·095)	0·97
All	52	1·045 (0·094)	0·557 (0·046)	0·70	63	1·127 (0·028)	0·525 (0·078)	0·96

[a]df = degrees of freedom for regression. A total of 54 datasets was used for constructing sequential sampling models.
[b]SE = standard error of the mean. Parameter estimates for the slope were not significantly different from 1 in any individual year or in the combined analysis ($P > 0·05$) in the model development datasets, but were greater than 1 in the model validation datasets. Intercept parameter estimates for the intercept parameter estimates were greater than 0 in all years and in the combined analyses ($P < 0·0001$).

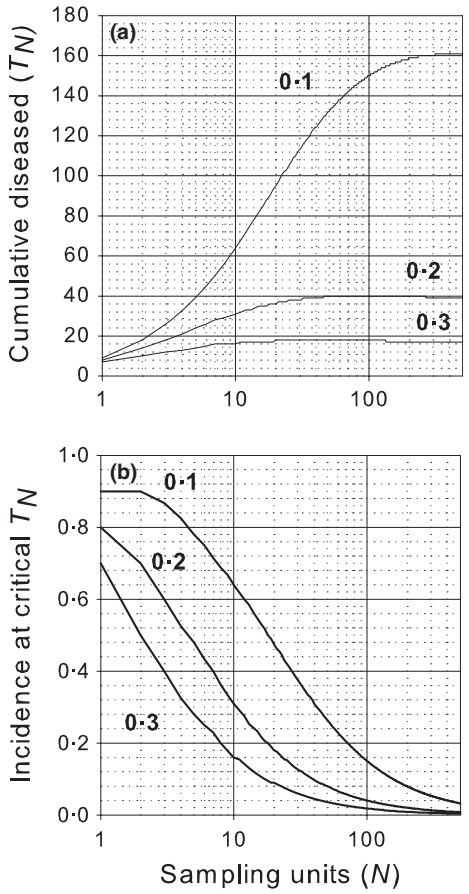

Figure 4 Sequential-estimation stop limits for estimating the mean incidence of bean pods with white mould (*Sclerotinia sclerotiorum*) with a coefficient of variation (C) of 0·1, 0·2 or 0·3. (a) Cumulative number of diseased pods (T_N) versus the total number of sampling units (N). (b) Mean disease incidence at critical T_N (the point where the observed cumulative number of diseased pods crosses the model T_N curve) in relation to N. Sampling ceases when the cumulative number of diseased pods crosses the critical T_N in (a), at which point mean disease incidence is then calculated as T_N/nN.

sequential sampling were very similar to the true disease incidence (Fig. 5a,b). However, this may be artefactual since the datasets were fully sampled (all 64 sampling units), and thus $\hat{p} = p$. Because of the small values of p, achieving the prespecified level of precision was not possible in any of the 65 datasets where $p > 0$ when C was set to 0·1 (Fig. 5c), and only six of the 65 datasets when $C = 0·2$ (Fig. 5). At $C = 0·1$, all 64 sampling units were evaluated in all of the datasets, while all but three of the datasets were completely sampled when $C = 0·2$ (Fig. 5e,f).

Bootstrapping evaluation

Bootstrap evaluation generally supported the observations of the simulated sampling. Disease incidence estimates were imprecise when $\hat{p}$ was low. The achieved C was greater than the prespecified C for datasets where $\hat{p} \leq 0·16$ when $C = 0·1$ (Fig. 6a) and $\hat{p} \leq 0·04$ when $C = 0·2$. The achieved C approached the prespecified C as $\hat{p}$ increased, and the median achieved C was less than the prespecified C for two datasets when $C = 0·1$, and six datasets when $C = 0·2$, as a result of the minimum sampling rule.

Although the prespecified precision was not attained in some instances, the estimates of $\hat{p} - p$ included zero for all datasets at both $C = 0·1$ and 0·2 (Fig. 6c,d), indicating that $\hat{p}$ was close to p for these datasets, but with the same caveat as noted above. Confidence intervals generally increased with increasing p because the sample size (N) decreased with increasing p for both levels of C (Fig. 6e,f). For $C = 0·2$, sample sizes were greatest for datasets where $p \leq 0·04$ (datasets 1 to 3) and in these datasets estimated $\hat{p} \approx p$.

Sequential classification

Sequential classification stop lines for the six sequential classification plans are shown (Fig. 7). Increasing α and β slightly reduced the distance between the stop lines (Fig. 7a,b), but had little effect on the steepness of the OC curves (Fig. 7c,d). As expected, the choice of the threshold p_t was much more influential to the OC than the error rates. The OC curve was flatter for the sampling plan with $p_t = 0·15$ than at lower values of p_t, indicating a greater classification error rate

Varying α and β had some effect on the ASN curves, which was most evident when p was near p_t, but again the choice of p_t was much more influential on ASN than the

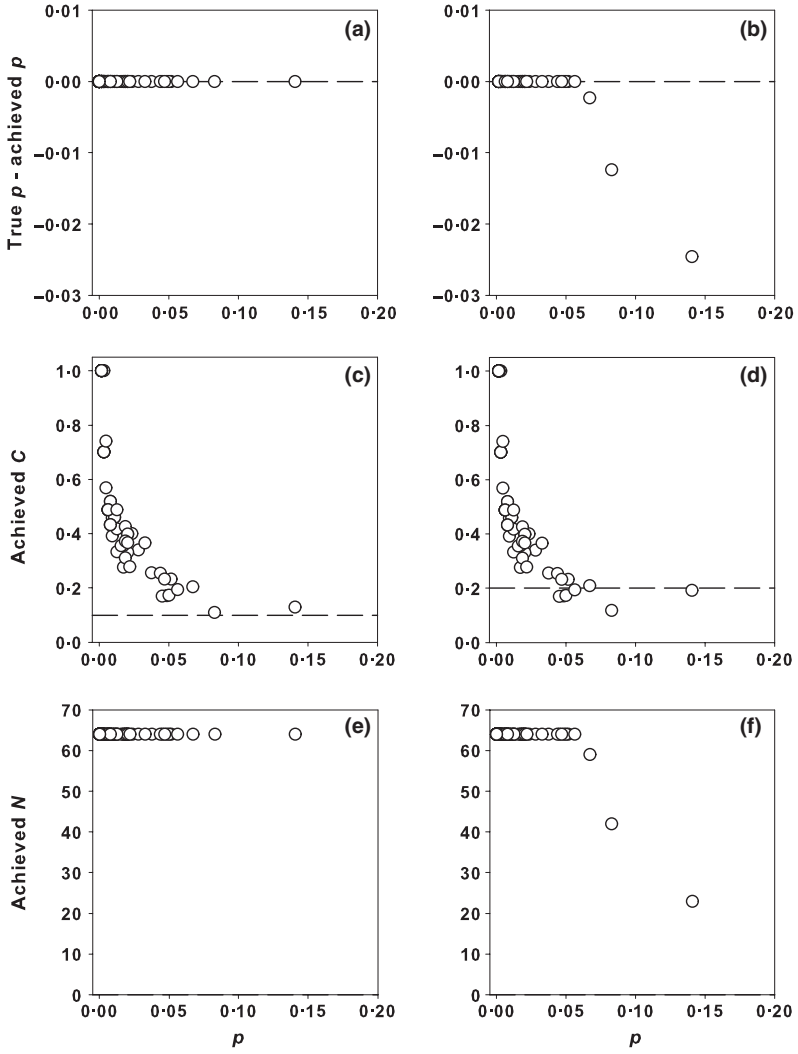

Figure 5 Validation of sequential sampling plans for estimating the incidence of bean pods with white mould (*Sclerotinia sclerotiorum*) in 65 commercial bean fields in Tasmania, Australia. (a and b) Relationship between true disease incidence *(p)* and estimated disease incidence ($\hat{p}$) from a sequential sample. (c and d) Relationship between true *p* and the achieved coefficient of variation (C). (e) and (f) Relationship between true *p* and number of sampling units (*N*) collected. (a, c and e) $C = 0{\cdot}1$; (b, d and f) $C = 0{\cdot}.2$. The dashed lines in (c) and (d) are the prespecified values of $C = 0{\cdot}1$ (c) and 0·2 (d). Datasets contained 64 sampling units located along four to five transects.

error rates. The ASN (rounded up to the nearest integer) at $p_t = 0{\cdot}03$, 0·05 and 0·15 was 35, 48, and 21 sampling units for $\alpha = \beta = 0{\cdot}05$, and 24, 31 and 16 sampling units for $\alpha = \beta = 0{\cdot}10$, respectively (Fig. 7e,f). The ASN was near or identical to the minimum sample size for all sampling plans when *p* was far ($\geq 0{\cdot}10$) from p_t.

Simulated sampling validation

At the three values of p_t and two combinations of error rates evaluated, correct decisions regarding classification of *p* were made at least 93% of the time when stop lines were generated, assuming a random (binomial) distribution of disease incidence (Table 3). Fewer misclassification errors occurred at the higher values of p_t. On average, 10–11·27 sampling units had to be evaluated to classify a dataset, the former value being equal to the minimum sampling rule that was imposed.

Correct decisions were made more often when the stop lines were generated assuming a beta-binomial (aggregated) distribution of disease incidence (Table 3). However, the slightly higher correct decision rate came at the cost of assessing more sampling units, on average 10·06–15·03 in total, depending on p_t.

Bootstrap evaluation

Again, changing p_t had a greater effect on the OC and ASN curves than did altering α and β. Increasing p_t flattened the OC curve and decreased the ASN, indicating an overall increase in the incorrect decision rate related to collection of fewer samples (Fig. 8). Bootstrap evaluation of the sampling plans indicated that the achieved OC and ASN were similar to the OC and ASN curves obtained by Monte Carlo simulation for the 12 datasets evaluated.

Discussion

This study has provided quantitative information on the spatial characteristics of white mould epidemics in Australian bean fields. Disease incidence varied widely both between and within fields, with a median over the study period of 8·4% in the model development datasets. The incidence of pods with white mould was characterized by

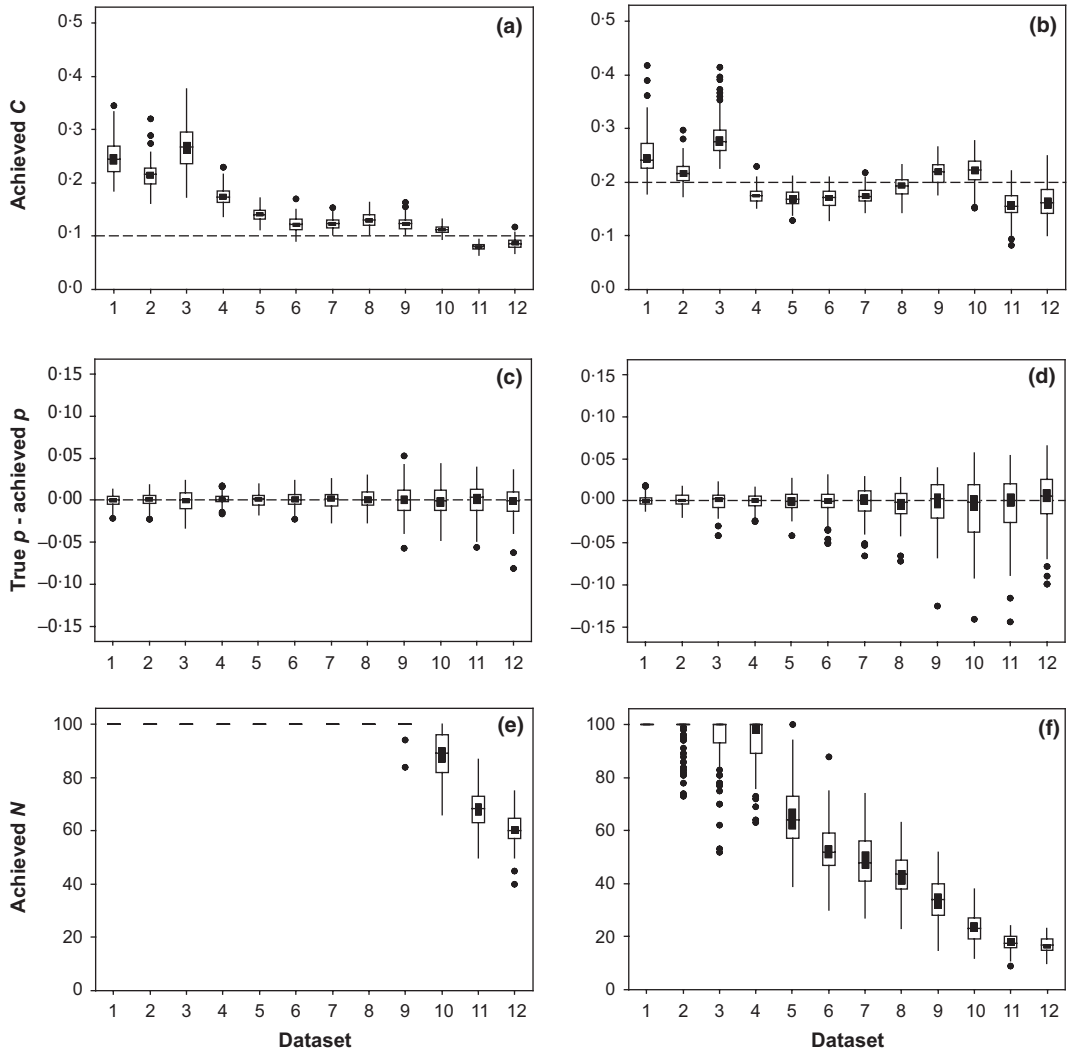

Figure 6 Box plots of the achieved coefficient of variation (C) (a and b); the difference between the true incidence (p) of pods with white mould (*Sclerotinia sclerotiorum*) and the estimated disease incidence ($\hat{p}$) based on sequential samples (c and d); and the achieved sample size (N) (e and f) from 100 bootstrap samplings of 12 datasets used for model evaluation. Preselected values of C are 0·1 (a, c and e) and 0·2 (b, d and f) and are indicated by dashed lines in (a) and (b). Sequential-estimation stop lines were generated with estimated binary power law parameters a = 0·194 and b = 1·045. The model evaluation datasets were chosen by selecting three datasets randomly from each of four disease incidence classes ($0{\cdot}01 < \hat{p} < 0{\cdot}02, 0{\cdot}02 \leq \hat{p} < 0{\cdot}04, 0{\cdot}04 \leq \hat{p} < 0{\cdot}08$, and $\hat{p} > 0{\cdot}08$) from among the 54 model construction datasets. The datasets are arranged in ascending order of $\hat{p}$. Datasets contained 100 sampling units selected along a single transect. Box plots show the median (line in open boxes), middle 50% of the data (open box), 95% confidence interval for the median based on the non-parametric sign-test (solid bar inside box), extremes of the data points (whiskers), and outliers (solid circles).

a largely random to slightly aggregated pattern of disease incidence at the scale of individual plants, with some patches of plants with similar disease levels on pods occurring at a scale of 1 m or greater. There are several biological processes that could result in such patterns. Random patterns of disease are characteristic of highly dispersible and/or well distributed inoculum (Turechek & Mahaffee, 2004). Small patches of sampling units with similar disease levels on pods were detected by correlation-based analyses, particularly when disease incidence was greater than on plants. Spatial analysis of the incidence of bean plants with white mould, as opposed to pods, was also conducted using disease data collected in 109 fields used for model validation, although that data was not presented here because of space limitations. However, that analysis indicated disease incidence was more aggregated on plants, with $\hat{\theta}$ varying from 0 to 1·73 with median 0·11, and D varying from 0·78 to 6·81 with median 1·96. Among the 80 fields where white mould was observed on plants, the corresponding estimated binary power law slope, $\hat{b}$, and intercept, $\ln(\hat{A}_x)$, parameters were 1·254 (SE = 0·032) and 1·086 (SE = 0·064), respectively. Although processes responsible for patterns cannot be deduced conclusively from this analysis, the

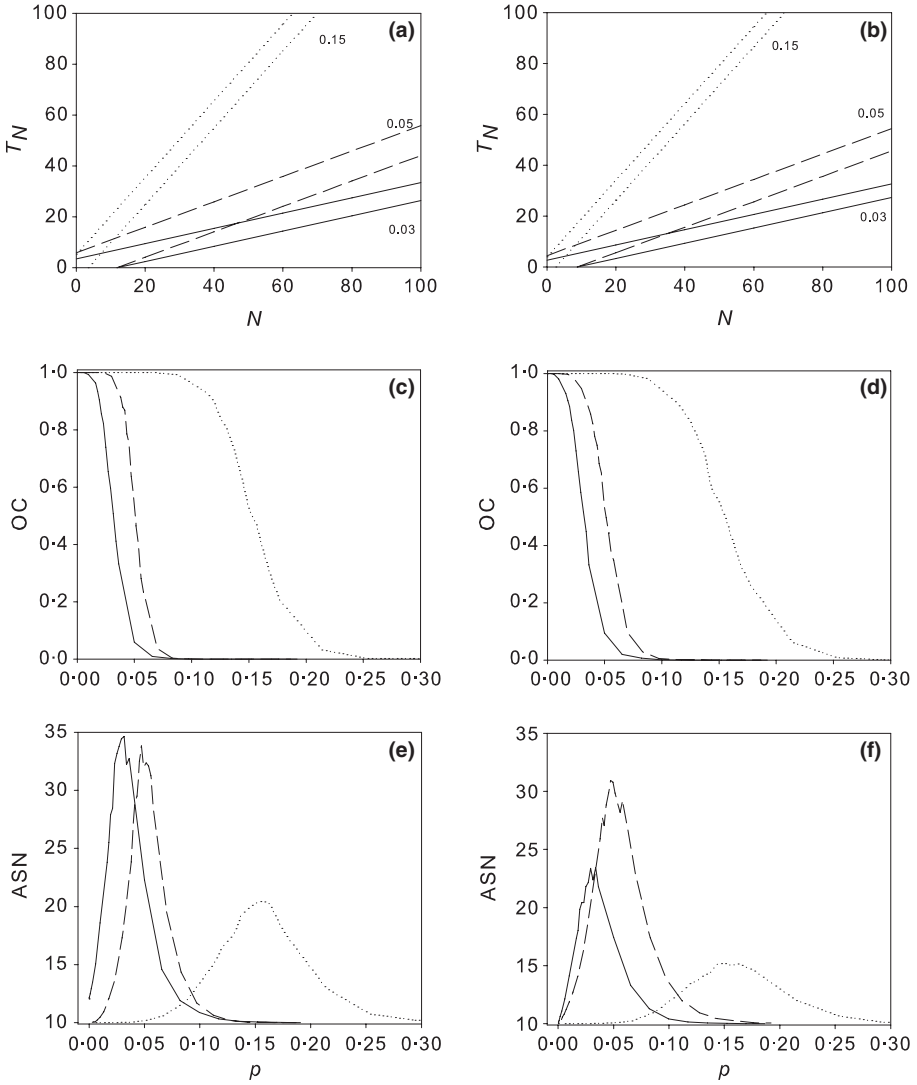

Figure 7 Stop lines for classifying the incidence of bean pods with white mould (*Sclerotinia sclerotiorum*) as above or below a critical threshold, p_t, from a cluster sample with n = 10 pods per sampling unit. (a and b) Stop lines based on Wald's sequence probability ratio test with p_0 = 0·01 and p_1 = 0·05 (p_t = 0·03), with p_0 = 0·03 and p_1 = 0·07 (p_t = 0·05), and with p_0 = 0·088 and p_1 = 0·214 (p_t = 0·15). (c and d) Operating characteristic (OC) curves and (e and f) average sample number (ASN) curves for sequential classification stop lines defined in (a) and (b). OC and ASN curves were determined by 1000 Monte Carlo simulations with the heterogeneity parameter as a function of disease incidence according to the binary power law, where a = 0·194 and b = 1·045. Type I (α) and type II (β) error rates were set at $\alpha = \beta$ = 0·05 in (a), (c) and (e) and $\alpha = \beta$ = 0·10 in (b), (d) and (f).

small-scale aggregation on pods in the model development datasets, but greater degree of aggregation on plants observed in this study may suggest localized spread of ascospores within bean fields. This is similar to the spatial characteristics of sclerotinia stem rot in soyabean (Gracia-Garza *et al.*, 2002) and sclerotinia flower blight in pyrethrum (Pethybridge *et al.*, 2010). Similarly, the absence of substantial inoculum contribution from ascospores outside the transect area of interest also suggests that diseased pods would be more likely to be identified in those areas of the fields where apothecia are found. Such an association between localized occurrence of apothecia and the incidence of pyrethrum flowers with sclerotinia flower blight was implied in this pathosystem (Pethybridge *et al.*, 2010). If inoculum is truly dispersed predominantly locally, this suggests that management efforts should be directed at reducing primary inoculum levels within individual fields, rather than focusing on a farm- or regional scale. Designed experiments are needed to test hypotheses on inoculum dispersal dynamics in this environment.

Spatial analyses of the epidemics also provided the foundation for developing statistically sound sampling approaches for estimating disease incidence or classifying disease incidence above or below the provisional industry threshold for crop rejection. The sampling plans

Table 3 Correct decision and error rates (proportion) of sequential classification plans for classifying the incidence of bean pods with white mould (*Sclerotinia sclerotiorum*) above or below varying disease incidence thresholds (p_t)

	p_t = 0·03[a]		p_t = 0·05		p_t = 0·15	
	α = 0·05	β = 0·1	α = 0·05	β = 0·1	α = 0·05	β = 0·1
Binomial						
Correct decision	0·93	0·93	0·96	0·95	1	1
Type I error	0·05	0·05	0·01	0·02	0	0
Type II error	0·03	0·03	0·03	0·03	0	0
Type I or II error	0·07	0·07	0·04	0·05	0	0
Mean *N*	11·27	10·40	11·26	10·53	10·06	10
Median *N*	10	10	10	10	10	10
Beta-binomial						
Correct decision	0·95	0·95	0·98	0·98	0·99	1
Type I error	0·02	0·02	0·00	0·00	0·01	0
Type II error	0·03	0·03	0·02	0·02	0	0
Type I or II error	0·05	0·05	0·02	0·02	0·01	0
Mean *N*	15·03	12·02	14·86	11·95	10·21	10·06
Median *N*	12	10	12	10	10	10

[a]Type I error indicates that mean disease incidence was incorrectly classified as $>p_t$; type II error indicates that mean disease incidence was incorrectly classified as $<p_t$, where p_t is a critical value of disease incidence. Mean and median *N* were calculated from all 109 model validation datasets. The parameters α and β were specified to control type I and type II error rates, respectively.

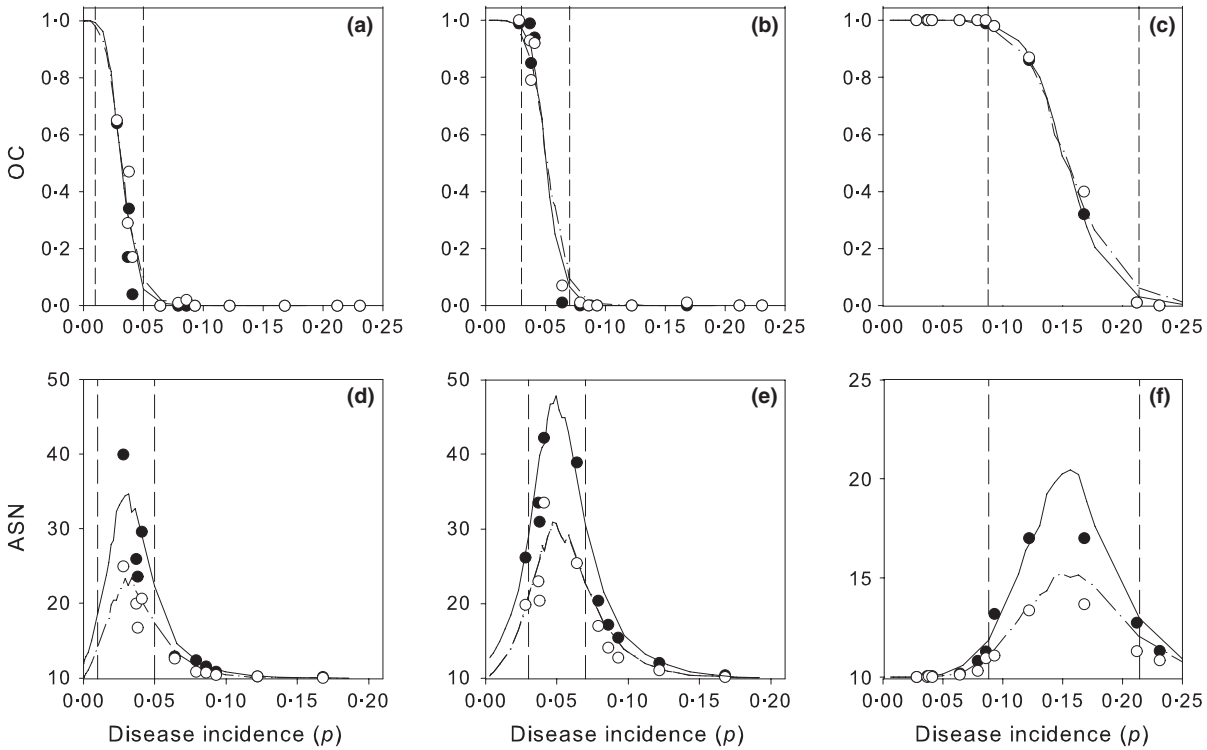

Figure 8 (a, b and c) Operating characteristic (OC) and (d, e and f) average sample number (ASN) curves for sequential classification sampling plans as determined by Wald's sequential probability ratio test for the incidence of bean pods with white mould (*Sclerotinia sclerotiorum*). Threshold values are: (a and d) p_0 = 0·01, p_1 = 0·05 and p_t = 0·03; (b and e) p_0 = 0·03, p_1 = 0·07 and p_t = 0·05; and (c and f), p_0 = 0·088, p_1 = 0·214 and p_t = 0·15. OC and ASN curves were determined by 1000 Monte Carlo simulations with the parameter a function of the mean disease incidence according to the binary power law, where a = 0·194 and b = 1·045. Curves with error probabilities of $\alpha = \beta$ = 0·05 (solid line) and $\alpha = \beta$ = 0·10 (dot-dashed line) are shown. Circles are the achieved OC and ASN from 100 bootstrap simulations of sequential sampling for classification of 12 model development datasets; open circles are simulations where $\alpha = \beta$ = 0·05, and solid circles are simulations where $\alpha = \beta$ = 0·10. The 12 datasets were chosen by selecting three datasets randomly from each of four disease incidence classes (0·02 < $\hat{p}$ < 0·04, 0·04 < $\hat{p}$ < 0·08, < 0·08 < $\hat{p}$ < 0·16, and $\hat{p}$ > 0·16) from among the 54 model development datasets.

developed in this research were not intended to inform decisions regarding application of control measures for the reasons discussed previously. Rather, the sampling plans were designed to quantify disease incidence on pods near harvest. The sequential estimation sampling plans tended to perform appropriately when disease incidence was at least 4%, which is near the provisional thresholds sometimes used by processors for crop rejection. To achieve a highly precise estimate of disease incidence ($C = 0{\cdot}1$), over 100 plants, with 10 pods sampled on each plant, would need to be evaluated when disease incidence is <8%. When precision requirements can be relaxed ($C = 0{\cdot}2$), the number of plants that need to be evaluated decreases with increasing disease incidence, to as few as 10. Given the stringent industry standards for white mould incidence on pods and practical considerations of the labour needed to conduct disease assessments, a lower level of precision, e.g. $C = 0{\cdot}3$, may need to be accepted to feasibly implement a sequential estimation plan.

For pest management, often only a classification of disease or pest status above or below some critical value for decision making is needed (Binns & Nyrop, 1992; Binns *et al.*, 2000). When only a classification of disease incidence is required, for research purposes or otherwise, the sequential classification plans developed herein appeared to provide a very useful tool for accurately classifying fields after inspection of relatively few sampling units. The sequential classification plans enabled disease incidence on pods to be classified correctly in at least 95% of fields after sampling only 10–15 plants.

The average sample size could be reduced even further by relaxing the minimum sampling rule of 10 plants used in the sampling plans developed here. White mould tends to be aggregated at scales larger than those considered in the current study, such as in low-lying areas or microclimates that favour extended periods of wetness on plants. Thus, the present study used a relatively stringent minimum sampling rule to increase the chance that such areas could be sampled. In practice, portions of fields with recurrent white mould may be the first areas where sampling should begin. Such 'targeted sampling' would minimize the risk of type II errors (i.e. incorrectly classifying a field as having disease incidence less than the disease threshold), which are probably more important to processors than type I errors.

A potential source of error in these studies is the assumption that disease assessments based on samples collected by research personnel are congruent with disease assessments by users of the sampling plans. Although estimates of disease incidence by the authors were correlated with disease incidence estimates by a co-operating processor, the former tended to to be greater than the latter. This may have been caused by differences in sampling scales (i.e. from across the field compared to estimates from truckloads), or from a proportion of bean pods infected by *S. sclerotiorum* being less robust (rotten) and broken up and left in the field during the harvesting process. The sequential sampling plan that used a classification threshold of 0·15 was designed to be calibrated, approximately, to what a processor may deem as 0·05 incidence of diseased pods. Although the OC curve was not as steep, indicating classification errors, this sampling plan performed adequately during validation. Correct decisions on disease status above or below the processor threshold were made at least 99% of the time after evaluation of, on average, only 10 plants. Given that assessment of white mould on pods can be very time consuming, implementation of one of the sampling plans developed in this work could substantially improve the efficiency and perhaps precision of current sampling methods.

Acknowledgements

This project was funded by Horticulture Australia Limited in partnership with AusVeg (project number VG07126; program 2·1) and USDA-ARS CRIS Project 5358-21000-035-00. We gratefully acknowledge the bean growers and processors who allowed access to their fields for sampling. Travel of Dr Gent to Australia was also partially funded by the University of Tasmania's Visiting Scholar Program. Thanks are also extended to Craig Palmer, Stacey Pilkington, Dr Jason Scott, Thomas O'Malley, Phillip Beveridge, Gordon Tuck, and Phil Gardam, University of Tasmania, for excellent technical assistance.

References

Abawi GS, Grogan RG, 1979. Epidemiology of diseases caused by *Sclerotinia* species. *Phytopathology* **69**, 899–904.

Abawi GS, Polach FJ, Molin WT, 1975. Infection of bean by ascospores of *Whetzelinia sclerotiorum*. *Phytopathology* **65**, 673–8.

Binns MR, Nyrop JP, 1992. Sampling insect populations for the purpose of IPM decision making. *Annual Review of Entomology* **37**, 427–53.

Binns MR, Nyrop JP, van der Werf W, 2000. *Sampling and Monitoring in Crop Protection: The Theoretical Basis for Designing Practical Decision Guides*. Wallingford, UK: CABI Publishing.

Boland GJ, Hall R, 1987. Epidemiology of white mould on white bean in Ontario. *Canadian Journal of Botany* **9**, 218–24.

Boland GJ, Hall R, 1988. Relationships between the spatial pattern and number of apothecia of *Sclerotinia sclerotiorum* and stem rot of soybean. *Plant Pathology* **37**, 329–36.

Clarkson JP, Phelps K, Whipps JM, Young CS, Smith JA, Watling M, 2004. Forecasting sclerotinia disease on lettuce: toward developing a prediction model for carpogenic germination of sclerotia. *Phytopathology* **94**, 268–79.

Dillard HR, Seem RC, 1990. Use of an action threshold for common maize rust to reduce crop loss in sweet corn. *Phytopathology* **80**, 846–9.

Gaunt RE, Cole MJ, 1992. Sequential sampling for wheat stripe rust management. *Crop Protection* **11**, 138–40.

Gent DH, Turechek WW, Mahaffee WF, 2007a. Sequential sampling for estimation and classification of the incidence of hop powdery mildew I: leaf sampling. *Plant Disease* **91**, 1002–12.

Gent DH, Turechek WW, Mahaffee WF, 2007b. Sequential sampling for estimation and classification of the incidence of hop powdery mildew II: cone sampling. *Plant Disease* **91**, 1013–20.
Gent DH, Turechek WW, Mahaffee WF, 2008. Spatial and temporal stability of the parameters of the binary power law. *Phytopathology* **98**, 1107–17.
Gracia-Garza JA, Boland GJ, Vyn TJ, 2002. Influence of crop rotation and reduced tillage on white mold of soybean caused by *Sclerotinia sclerotiorum*. *Canadian Journal of Plant Pathology* **24**, 115–21.
Hoffman MP, Nyrop JP, Kirkwyland JUJ, Riggs DM, Gilrein DO, Moyer DD, 1996. Sequential sampling plan for use in scheduling control of lepidopteran pests for fresh market sweet corn. *Journal of Economic Entomology* **89**, 386–95.
Huang HC, Kozub G, 1993. Influence of inoculum production temperature on carpogenic germination of sclerotia of *Sclerotinia sclerotiorum*. *Canadian Journal of Microbiology* **39**, 548–50.
Hughes G, Madden LV, 1992. Aggregation and incidence of disease. *Plant Pathology* **41**, 657–60.
Hughes G, Madden LV, Munkvold GP, 1996. Cluster sampling for disease incidence data. *Phytopathology* **86**, 132–7.
Koike ST, Gladders P, Paulus AO, 2007. *Vegetable Diseases – A Color Handbook*. Burlington, MA: Academic Press.
Madden LV, Hughes G, 1994. BBD-computer software for fitting the beta-binomial distribution to disease incidence data. *Plant Disease* **78**, 536–40.
Madden LV, Hughes G, 1995. Plant disease incidence: distributions, heterogeneity, and temporal analysis. *Annual Review of Phytopathology* **33**, 529–64.
Madden LV, Hughes G, 1999. Sampling for plant disease incidence. *Phytopathology* **89**, 1088–103.
Madden LV, Louie R, Abt JJ, Knoke JK, 1982. Evaluation of tests for randomness of infected plants. *Phytopathology* **72**, 195–8.
Madden LV, Hughes G, Munkvold GP, 1996. Plant disease incidence: inverse sampling, sequential sampling, and confidence intervals when observed mean incidence is zero. *Crop Protection* **15**, 621–32.
Madden LV, Hughes G, van den Bosch F, 2007. *The Study of Plant Disease Epidemics*. St Paul, MN: APS Press.
Malloy OC, 1993. *Plant Disease Control: Principles and Practice*. New York, NY: John Wiley and Sons.
McCartney HA, Lacey ME, 1991. The relationship between the release of ascospores of *Sclerotinia sclerotiorum*, infection and disease in sunflower plots in the United Kingdom. *Grana* **30**, 486–92.
McDonald MR, Boland GJ, 2004. Forecasting diseases caused by *Sclerotinia* spp. in eastern Canada: fact or fiction? *Canadian Journal of Plant Pathology* **26**, 480–8.
Pethybridge SJ, Hay FS, Gent DH, 2010. Characterization of the spatiotemporal attributes of sclerotinia flower blight in a perennial pyrethrum pathosystem. *Plant Disease* **94**, 1305–13.
Phillips AJL, 1987. Carpogenic germination of sclerotia of *Sclerotinia sclerotiorum*: a review. *Phytophylactica* **19**, 279–83.
Ryan B, Joiner B, Cryer J, 2005. *Minitab Handbook*, 5th edn. Belmont, CA: Brooks/Cole.
Schwartz HF, Steadman JR, 1978. Factors affecting sclerotium populations of, and apothecium production by, *Sclerotinia sclerotiorum*. *Phytopathology* **68**, 383–8.
Turechek WW, Mahaffee WF, 2004. Spatial pattern analysis of hop powdery mildew in the Pacific Northwest: implications for sampling. *Phytopathology* **94**, 1116–28.
Turechek WW, Ellis MA, Madden LV, 2001. Sequential sampling for incidence of phomopsis leaf blight of strawberry. *Phytopathology* **91**, 336–47.
Turkington TK, Morall RAA, 1993. Use of petal infestation to forecast sclerotinia stem rot of canola: the influence of inoculum variation over the flowering period and canopy density. *Phytopathology* **83**, 682–9.
Vincelli PC, Lorbeer JW, 1987. Sequential sampling for timing initial fungicide applications to control botrytis leaf blight of onion. *Phytopathology* **77**, 1301–3.
Willetts HJ, Wong JAL, 1980. The biology of *Sclerotinia sclerotiorum, S. trifoliorum,* and *S. minor* with emphasis on specific nomenclature. *The Botanical Review* **46**, 101–65.
Wong JAL, 1978. Green beans and white mould. *Tasmanian Journal of Agriculture* **49**, 195–201.